GSJ: Volume 9, Issue 2, February 2021, Online: ISSN 2320-9186
www.globalscientificjournal.com

# VOLTAGE STABILITY STUDIES OF PHED IN IKWERRE ROAD DIOBU AXIS OF PORT HARCOURT, NIGERIA

[1]Albert Ehimhen Eigbe, [2]Prof. Christopher Okwuchukwu Ahiakwo, [3]Dr. Sepiribo Lucky Braide

*[1] Research student, Electrical Engineering Department, Rivers State University, Port Harcourt, P.M.B. 5080, Rivers State, Nigeria. E-mail: aeeigbe@yahoo.com*
*[2,3] Lecturer, Electrical Engineering Department, Rivers State University, Port Harcourt, P.M.B. 5080, Rivers State, Nigeria.*

**KeyWords**

Distributed Generator, ETAP, Fast Decoupled Load Flow, Load flow analysis, Newton-Raphson, Voltage stability

**ABSTRACT**

In this research, numerical iterative techniques were used to conduct voltage stability analysis of Port Harcourt Electricity Distribution (PHED) in Ikwerre Road, Diobu axis of Port Harcourt in Nigeria, with the view of addressing the system overload on the power system components such as transformer, undersize cable/conductor bus bar feeder links, etc. The application of reactive power support by capacitor compensation can help minimize the cost of distribution loss in the power supply to Ikwerre Road, Diobu axis Port Harcourt. The objectives focus on the following areas: compensation of capacitor bank before penetration to improve the system reliability, penetration of voltage stability indices values with different Distributed Generator (DG) size, increasing the DG size on voltages of different load point, increasing the DG size of power flow with different DG and without DG size, increasing the DG size as a result of maximum loading point, increasing the DG size on the penetration level from the Load, increasing the DG size on power losses. The tendency of studying the analysis of voltage instability in power system operation and planning is to strongly identify, monitor, plan, and predict the gradual increase in power system demand and voltage profile of the Ikwerre Road, Diobu axis of Port-Harcourt. Electrical Transient Analyzer Program (ETAP) software was used for the simulation of the system. The simulation of the existing system case shows inequality and overload conditions on the system components. From the simulation, it showed that increasing the size of DG unit on power flow causes a reduction in real power generated by The Power Holding Company of Nigeria (PHCN) due to the installed DG unit at Gambia street, Port Harcourt. Also, the maximum value of the loading parameter of the power system increased when the size of DG increases. Maximum load ability changes from 3.1217 to 4.0125 when the DG generates 60% from the load, thus the increase is by 0.8908. The increment in the value of Maximum load ability is due to the install DG. The results also showed that Reduction in the cost of power distribution and consumption in the network improves the system voltage profile and power system quality.

## 1. INTRODUCTION

In the past 40 years, the generation of electric power in Nigeria is through gas, oil, hydro, coal-fired power plants, but there are efforts to progress toward renewable and hybrid power generation. Even though new techniques are emerging, there is a need to maintain and properly manage the existing power supply networks, which are in a state of inadequate maintenance. The gradual migration of people from rural areas to urban cities has greatly increased the consumption pattern of electricity from the generating station to the end-users. Power system planners and operators are faced with issues related to voltage and power outages because the power system is constantly operated within or close to the stability limits [1] [2] [4].

Voltage instability has a progressive decay nature in the voltage magnitude, which can loss of load, transmission lines tripping, and can eventually lead to voltage collapse or blackout [5]. Normally, no power system can transfer an unlimited amount of electrical power to load but the deplorable state of power plants in the country has added to the problem of voltage instability, thus contributing to the epileptic power delivery in Nigeria. One of the major causes of voltage inability is the power system's inability to meet the reactive power demands in the stressed and overloaded power system to maintain desired voltages. Every component in the power system works at a certain voltage. If the component's voltage limit is exceeded, then damage to the equipment occurs and with lack of maintenance, the damage occurs faster [1] - [4] [8]. Voltage instability threatens the security, stability, and reliability of power systems and affects the socio-economic development of Nigeria because many people depend majorly on a steady electric power supply for activities in industry, healthcare, education, businesses, etc. it is necessary to confront the challenges to the actualize stable power supply in term of reliable and efficient delivery to the end-users [1] – [6].

The power supply to the Ikwerre road is plagued by overloading, and not frequently maintained, which resulted in a drastic drop in voltage profile and losses in power transmission and distribution from Afam to Ikwerre Road injection substation to consumers. This research carried out Voltage stability analysis of Port Harcourt Electricity Distribution (PHED) to Ikwerre Road, Diobu axis of Port Harcourt, Nigeria. One way of support used is by applying for reactive power support through capacitor compensation and implementing distributed generator (DG) to improve power system quality and voltage profile and help minimize the cost of distribution loss in the power supply of Ikwerre Road, Diobu axis, Port Harcourt. A Power flow study gave information on various buses voltages, phase angles, active power, and reactive power of the system. The research also highlighted the margin of safety for determining the possibility of feeder bus voltage collapse or breakdown in the network, in line with the statutory regulatory practice of IEEE code (that is, the operating or nominal voltage should not deviate from the tolerable limits of ±10%, or 0.95*pu* – 1.05*pu*, of the declared set values). The results of the research could provide Power Holding Company of Nigeria (PHCN) system operators, and other operational utilities the information to mitigate instability condition of the buses, lines, transformers, circuit breakers, etc., to have plans to avoid total system collapse and outages and to the actualization of reasonable power supply in term of reliable and efficient delivery to the end-users.

## 2. LITERATURE REVIEW

The modern electric power system network is a large and complex engineering system whose healthy existence is vital to the socio-economic development of man and its environment. The Power Holding Company of Nigeria (PHCN) consists of 6 Generation Companies (GENCOs), 1 Transmission Company of Nigeria (TCN), and 11 Distribution Companies (DISCOs). As shown in Table 1, the generating stations give a total installed generating capacity of 6500MW. The transmission network is made up of 5000km of 330KV lines, 6000km of 132KV lines, 23km of 330/132KV sub-stations, and 91 of 132/33KV substations. The distribution sector is comprised of 23.753km of 33KV lines 19,226km of 11kv lines, 679 of 33 and 11KV sub-stations. There are also 1790 distribution transformers and 680 injection substations. Since the 1950s, power stations in Nigeria are in operation, but there is poor delivery of electric power to consumers around the country due to the deteriorated state of these power plants and high-power demand. Presently, most of the generating units' have broken down due to limited available resources to carry out the needed maintenance. Although, the installed capacity of the existing power stations is 6500MW the maximum load ever "Recorded was 4,000MW. The transmission lines are radial and are overloaded. The switchgear is obsolete while power transformers have not been maintained for a long time. These networks are characterized by many disturbances which cause various hindrances and outages. The epileptic state of the power supply is grossly inadequate to meet the demand of electricity consumers in the country [1] [2] [4] [7] [8].

**Table 1: Power Stations in Nigeria**

| S/No | Power Station Name | Location/State | Status | Capacity (MW) |
|---|---|---|---|---|
| 1 | Egbin Thermal Power Station | Lagos | Operating | 1320 |
| 2 | Afam. Thermal PS | Rivers | Operating | 969,6 |
| 3 | Sapele Thermal PS | Delta | Operating | 1020 |
| 4 | Ijora Thermal PS | Lagos | Operating | 40 |
| 5 | Delta Thermal PS | Delta | Operating | 912 |
| 6 | Kainji Hydro PS | Niger | Operating | 760 |
| 7 | JebbaHvdro PS | Niger | Operating | 578 |
| 8 | Shiroro Hydro PS | Niger | Operating | 600 |
| 9 | AES Thermal PS | Lagos | Operating | 300 |
| | | | **TOTAL CAPACITY** | **= 6500** |

Source: PHCN National Control Center Oshogbo Daily Operational Report (2012)

### *A. Voltage Stability*

According to [3], Voltage stability or load stability refers to the ability of a power system to sustain satisfactory voltages in all its bus in standard operating conditions even after interruption or disturbance in the system. The voltage of a power system is stable under normal conditions, but when the system has faults or is disturbs, the voltage becomes unstable, leading to a gradual and uncontrollable decrease in voltage. Voltage stability is classified depending on the nature of disturbance that occurs in the system into small disturbance voltage stability and big disturbance voltage stability [3] [9]. Figure 1 shows the classification of voltage stability.

Voltage instability in most cases contributes to voltage collapse, which is a process by which voltage instability provides advantages of a low voltage profile in the essential part of the system. Voltage collapse can cause partial or total black-out, inefficient power supply to the respective consumers via designated feeder buses [3] [9]. The voltage stability limit refers to the operating limit in the power system above which no amount of injection of reactive power can restore the voltage of the system to its normal state. However, the reactive power injection can only change the system voltage until the reliability of the system voltage is preserved. The distribution grid regularly experiences system collapse when the system is overloaded beyond its boundary limit [3]. In general, causes of voltage instability include but not limited to the following

i. The inability for the system to meet high demands for power to give the ever-increasing loads/consumers
ii. Damage to the voltage regulator units
iii. Exceeding the voltage limit of equipment
iv. Unstable speed of the engine of the generator set

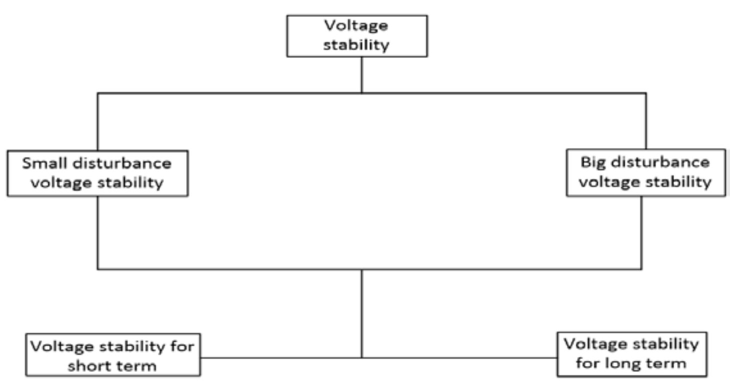


**Figure 1: Classification of Voltage Stability**

Compensation provides a veritable way to reduce the excess voltage/current to avoid damage to the utility centres. Compensation in the power system becomes very essential since the power flow problem is the computation of voltage magnitude and phase angle at each bus in a power system under balanced three-phase steady-state conditions [6] [13] [15]. Power system analysts have described power outage and voltage instability as commonly occurring events that have widely been studied by many power system researchers.

In [6], FACTS controllers are incorporated into the power system by using Static var compensators (SVC) and a thyristor controlled series compensator (TCSC) in OPF formation to assess the overall voltage stability of a multi-bus power system to achieve optimal power flow at different operating conditions and to assist system operators to select suitable FACTS device depending on the voltage stability related problems. In [9], a decentralized adaptive scheme emergency control scheme was proposed to actuate countermeasures when there is a threat of voltage collapse. The work used intelligent agents to monitor extend of disturbance in load voltage and generator reactive power and identify risks and initiate timely emergency response countermeasures which save the power system from complete voltage collapse. In [10] proposed a Whale optimization algorithm (WOA)-based method for an event-driven emergency demand response (EEDR) strategy to effectively improve voltage stability. WOA is a swarm Artificial Intelligence (AI) technique that mathematically models the pattern of foraging found in humpback whales [10] [11]. The authors used the WOA method to determine the optimal locations and amounts of load reductions to maintain voltage stability margin in an acceptable range during emergency operation of the power system [11]. Often, single DG placement may be sufficient for the power distribution system, and multiple DGs may be integrated into the power distribution network. The integration of DGs in the distribution system required optimal placement and sizing of DGs to yield minimum power losses and improved voltage profile. As a result, the optimal location of multiple DGs in the power distribution system is very important. In [12], the Particle Swarm Algorithm was proposed for the optimal location of multiple Distributed Generators (DGs) into the power distribution network for power loss minimization. Other researchers studied power or load flow analysis because it is an important tool to help mitigate problems related to voltage instability [13]

### *B. Flow analysis*

In a power system, power flows from generating station to the load through different branches of the network. Thus Load flow analysis is an essential pre-requisite for power system studies, and it is used to determine the steady-state operation of a power system. Also, the power flow analysis is a systematic mathematical approach that gives information about bus voltage, voltage magnitude, and phase angles, active and reactive power that flow through different branches, generators transformer setting, and load under steady-state conditions [13] – [16]. Researchers have proposed methods for the determination of these parameters that constitutes the solution to load flow problems.

The authors in [17] suggested increasing the reactance loading will give an increased voltage regulation for Load Flow Analysis on IEEE 30 Bus Systems using Newton-Raphson's (N-R) algorithm or Gauss-Seidel (G-S) method to solve the load flow problems and voltage instability. In [14], methods for conduction Load flow analysis include the Z-bus method, N-R algorithm, G-S methods, Fast Decoupled (F-D) algorithm. Also, Backward/forward sweep-based methods and loop impedance methods utilize branch currents or branch powers as state variables to solve the power flow problem. Load flow analysis with MATLAB software was carried out in [16] using N-R, F-D, and G-S methods. Comparison of the two methods shows G-S method ease in the analysis programming and has the most efficient use of core memory than the N-R method, but analysis of larger networks, N-R method is faster, more accurate, and more reliable. However, F-D has higher speed and better memory use. In [18], perturbation theory was utilized for the load analysis and the method attempts to enhance the convergence rate by partially linearizing the power flow equation with a focus on the voltage magnitude and the phase angle in each iteration. The technique gives faster, smarter, and more accurate results having tested the technique on the IEEE 5-bus, 14-bus, 30-bus, and 118-bus system than the conventional G-S technique of load flow calculation. In [19] load flow analysis was investigated for the performance of the electrical system during normal and abnormal operating conditions. Using ETAP to simulate, plan and coordinate distribution system, the information needed to optimize circuit usage, develop practical voltage profiles, minimize losses, etc. were provided.

Load balance among the components of power transmission and distribution networks is very important to reduce loss and overloading of components [4] [13]. To improve power transfer capability, performance and efficiency, in terms of transmission and distribution, adequate supports from the pro-creative power components is needed. The supports are achievable when the power system behaviour in terms of voltage and power flows in the electric network is determined for a given set of loading and operating systems constraints conditions.

## 3. MATERIALS AND METHOD

### *A. Description of the Supply Network*

The public power supply network is from the Afam power generating station via 132kV transmission line to 11kV and 33kV injection distribution lines that feed the Ikwerre road, Diobu, Port Harcourt, Rivers State, Nigeria. For use at the consumers' level, the 11kV and 33kV primary voltages are stepped down further to 415V and 220V respectively. The power system consists of a mixture of a single radial system and a parallel system that feed consumers and interconnect substations as shown in Figure 2. The power supply is transmitted to different areas in the Diobu area through major power transformers namely: Abel Jumbo S/S (Oil type Transformer 500 kVA – 11/0.433kV), Gambia Street S/S (Transformer 500 kVA – 11/0.433kV), Ihidionma S/S (Analysis of 11/0.415kV, 500kVA Power Transformer), Lumumba S/S (500 kVA Power Transformer), Akokwa Street S/S (Analysis of 11/0.415kV, 500kVA Power Transformer) and Emenike S/S (500 kVA Power Transformer).

## *B. Materials*

This research work considered the voltage stability studies particularly to Ikwerre Road, Mile 1, Diobu axis of Port Harcourt, with the application of load flow equation, voltage equations for the analysis of the 11kV Distribution network. Due to the nature of this work, physical investigation and collection of data were conducted to identify the issues related to voltage stability in the power supply units that feed the Ikwerre road, Diobu Axis, Port Harcourt, Nigeria. Some of the materials used in the execution of this research include but not limited to the following:

i. Data from the power supply network feeding the Ikwerre road area were collected, which include consumers' number on each transformer, losses on the Distributed generator (DG), output voltages, voltage profile on feeder buses, cross-section area of conductors, transformer profile, line profile.

ii. Observations from the investigation showed load flow analysis account for losses (MW, MVAR) from the sending to receiving-end and a consistent check is needed for purpose of compensation and improvement. Losses experienced in the designated buses: 20, 21, 23, 32, & 33 respectively, especially when power was injected into the area. The network is highly overloaded resulting in the drastic drop in voltage profile and excessive loss of power transmitted from Afam to Ikwerre Road injection substation to load ends. The power transformers at the injection substation are operating at a critical level. Due to the size and length of the feeder lines, together with the overloading condition, a considerable amount of voltage and power ($I^2R$) is lost.

iii. Electrical Transient Analyser Program (ETAP) version 12.6 platform was the simulator used in this research

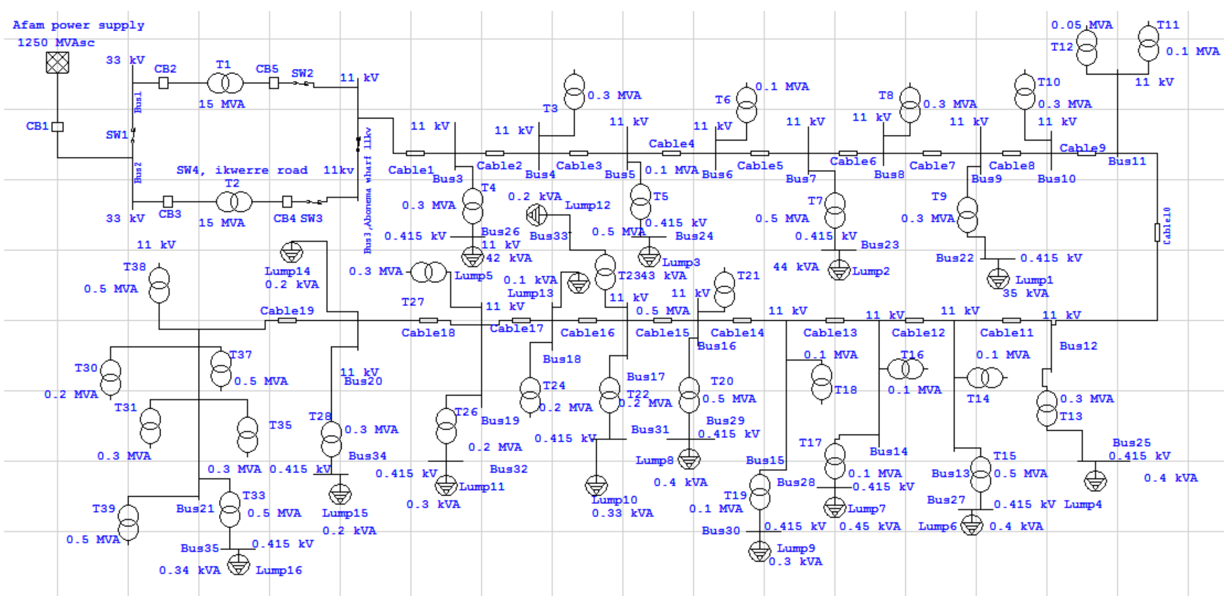


**Figure 2: Power supply system to the Ikwerre Road, Diobu, Port Harcourt (uncompensated)**

## *C. Methods*

Numerical iterative techniques are used in the research. The method for the load flow analysis is the embedded N-R method - an extension of the N-R technique embedded with Fast Decoupled Load Flow (FDLF) formulation. Load flow equations are essentially non-linear algebraic equations, which have to be solved through iterative numerical techniques - by starting with assumed values of known variables and obtaining successive better values of the same variable by repeated cycles of solution. The proposed method for the voltage stability studies were Load Tap Changing (LTC) and Optimal Capacitor Placement (OCP), which are optimization techniques. The OCP is to minimize the cost of the system. Ideally, the voltage magnitude statutorily should lie between $0.95 \leq |V_i| \leq 1.05pu$, and the angle should be very small for a balanced steady-state 50Hz power station to achieve effective operation. In the techniques, the base solution is obtained using the embedded N-R method, and then the bus voltage ranges out-side ±10% of the normal values (i.e. 0.95 to 1.05) per unit are checked to identify the problems. Table 2 shows The initial rating of the installed DG showing active and reactive power for 10% to 60% load.

**Table 2: Rating of active and reactive power with % Load**

| Rating of the load | Active Power (MWatt) | Reactive Power (MVAR) |
|---|---|---|
| 10% of the load | 0.3312 | 0.21 |
| 20% of the load | 0.427 | 0.39 |
| 30% of the load | 1.023 | 0.52 |
| 40% of the load | 1.121 | 0.81 |
| 50% of the load | 1.532 | 1.02 |
| 60% of the load | 2.223 | 1.09 |

With consideration to Figure 3(a), the admittance matrix for the *n* number bus system is given by Equations (1) and (2). The indices for load analysis on feeder and transformer are expressed in Equation (3) to (9). Considering Fig 3(b) and Fig 3(c), indices for shunt capacitor compensation are given by Equation (10) to (13).

$$Y_{Bus} = Y_{i\,k} = \begin{bmatrix} Y_{11} & Y_{12} & \dots & Y_{1n} \\ Y_{12} & Y_{22} & \dots & Y_{2n} \\ \vdots & \vdots & \dots & \vdots \\ Y_{n1} & Y_{n2} & \dots & Y_{nn} \end{bmatrix} \tag{1}$$

$$Z_{Bus} = Y_{Bus}^{-1} = \frac{Adj\ Y_{Bus}}{|Y_{bus}|} \tag{2}$$

$$\%\,Loading\ of\ feeder = \frac{average\ \ current\ \ on\ feeder}{maximum\ \ allowable\ \ current} \times 100 = \frac{active\ \ power\ \ demand\ \ on\ feeder}{maximum\ \ allowable\ \ Active\ load\ on\ feeder} \times 100 \tag{3}$$

$$\%\,P_D = \frac{average\ \ current\ \ on\ feeder}{60} \times 100 \tag{4}$$

$$V_D = E_s - V_r = I^f\,Z \tag{5}$$

$$\%\,V_D = \frac{V_D}{E_s} \times 100 \tag{6}$$

$$\%L^T = \frac{I_R + I_Y + I_n}{3\,I_n} \times 100 \tag{7}$$

$$CLD = TC\ \times\ \%L^T \tag{8}$$

$$V_2 = \frac{V_1\,N_2}{N_1} \times E_1\,K \tag{9}$$

$$T_1 = (P^2 + U_1^2)^{1/2} \tag{10}$$

$$T_2 = (P^2 + U_2^2)^{1/2} = (P^2 + (\,(U_1 - U_C)^2)^{1/2} \tag{11}$$

$$pf_1 = \cos\theta_1 = \left(\frac{P}{T_1}\right) = \frac{P}{(P^2 + U_1^2)^{1/2}} \tag{12}$$

$$pf_2 = \cos\theta_2 = \left(\frac{P}{T_2}\right) = \frac{P}{(P^2 + (\,(U_1 - U_C)^2)^{1/2}} \tag{13}$$

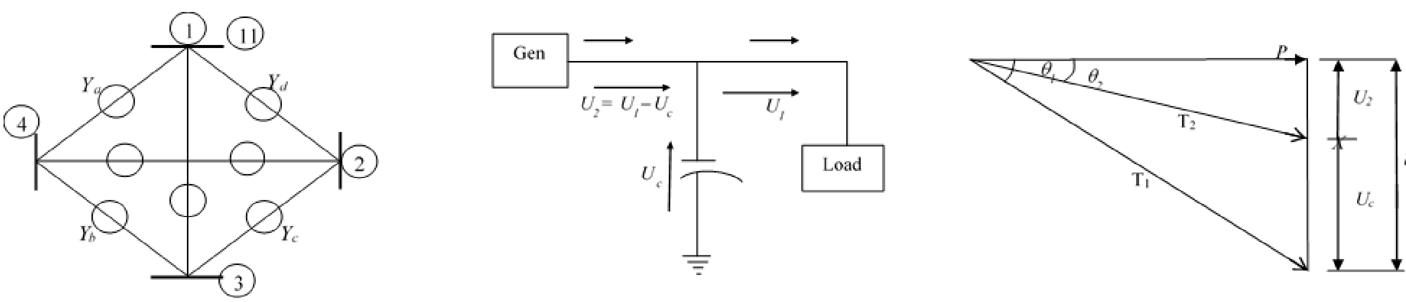


**Figure 3: (a) Four bus system diagram (b) Capacitor compensation diagram (c ) Pythagoras theorem for capacitor compensation (capacitor bank)**

The power system line parameters are expressed in Equation (14) to (19). The basic indices for load flow analysis are expressed in Equations (20) to (23). The objective function (i.e. cost of OCP) and voltage instability are given by Equation (24) and (25) respectively. The angle instability is expressed in Equation (26) and (27)

$$R_o = \frac{1000\ \pounds}{A}\ (\Omega/km) \tag{14}$$

$$r = \sqrt[2]{\frac{A}{\pi}}\ (m) \tag{15}$$

$$x_o = 0.445\ \frac{D_{GMD}}{r} + 0.0157 \quad (\Omega/km) \tag{16}$$

$$b_o = 7.58 \times \frac{1}{\log\left(\frac{D_{GMD}}{r}\right)} \quad (\Omega/km)^{-1} \tag{17}$$

$$D_{GMD} = \sqrt[3]{(D_{RB}\ D_{RY}\ D_{BY})} \qquad For\ a\ single\ circuit \tag{18}$$

$$D_{GMD} = \sqrt[3]{2(D^3)} = D\ \sqrt[3]{2} = 1.26\ D \qquad For\ overhead\ conductors\ arranged\ horizontally \tag{19}$$

$$I_i = \sum_{k=1}^{n} Y_{i\,k}\, V_k \tag{20}$$

$$S_i^* = P_i + j\,Q_i = V_i^*\, I_i = V_i^* \sum_{k=1}^{n} Y_{i\,k}\, V_k \qquad i = 1, 2, \ldots .n \tag{21}$$

$$P_i = |V_i| \sum_{k=1}^{n} ( |Y_{i\,k}|\, |V_k| \cos(\theta_{i\,k} + \delta_k - \delta_i )) \tag{22}$$

$$Q_i = |V_i| \sum_{k=1}^{n} ( |Y_{i\,k}|\, |V_k| \sin(\theta_{i\,k} + \delta_k - \delta_i )) \tag{23}$$

$$Objcetive\ funtion = \sum_{i=1}^{N_{best}} (x\, C_{oi} + T_{ci}\, C_{ci} + B_i\, C_{2i}\, M ) + C_E \sum_{i=1}^{N_{best}} M_1\, P_L^1 \tag{24}$$

$$V_{stab} = \sqrt{\frac{(E^2 - 2Q_L\, X) - (2Q_L X - E^2)^2 - 4X^2(Q_L^2 - P_L^2)}{2}} \tag{25}$$

$$P_L = \frac{E_s\, V_r}{X} \sin \emptyset \tag{26}$$

$$\emptyset = \sin^{-1}\left(\frac{P_L\, X}{E_s\, V_r}\right) \tag{27}$$

The FDLF analysis and Jacobian elements are expressed in Equation (28) to (38). While the Power Flow Injections and Jacobian Elements are given by Equation (39) to (50).

$$\left.\begin{array}{r} V_i = -|V_i|\, e^{j\delta i} \\ V_i^* = |V_i|\, e^{-j\delta i} \\ V_k = -|V_k|\, e^{j\delta k} \\ Y_{i\,k} = |Y_{i\,k}|\, e^{-j\theta_{ik}} \end{array}\right\} \qquad For\ a\ given\ i - th\ bus \tag{28}$$

Then, $P_i = |V_i|\, |V_{ii}|\, |Y_{iii}| \cos\theta_{ii} + \sum_{\substack{k=1 \\ i\neq 1}}^{n} (|V_i|\, |V_k|\, |Y_{ik}|\, \cos(\theta_{ik} + \delta_i - \delta_k))$ *i* = 2,3,4,…*n* (29)

$$Q_i = |V_i|\, |V_k|\, |Y_{ii}| \sin\theta_{ii} + \sum_{\substack{k=1 \\ i\neq 1}}^{n} (|V_i|\, |V_k|\, |Y_{ik}|\, \sin(\theta_{ik} + \delta_i - \delta_k)) \tag{30}$$

$$\begin{bmatrix} \Delta P \\ \Delta Q \end{bmatrix} = \begin{bmatrix} J_{1ik} & 0 \\ 0 & J_{4ik} \end{bmatrix} \begin{bmatrix} \Delta\delta \\ \Delta v/_{v} \end{bmatrix} \tag{31}$$

$$\Delta P = J_1\, \Delta\delta \qquad \text{and} \qquad \Delta Q = J_4\, \frac{\Delta v}{v} \tag{32}$$

$$J_{1ik} = J_{4ik} = -|V_i|\, |V_k|\, |Y_{ik}| \qquad for\ k \neq i \tag{33}$$

$$J_{1ik} = J_{4ik} = -|V_i|^2\, B_{ii} \tag{34}$$

$$\Delta P_i = J_1\, \Delta\delta = |V_i|\, |V_k|\, B_{ik}\, \Delta\delta_k \quad (35)$$

$$\Delta Q_i = J_4\, \frac{\Delta v}{v} = |V_i|\, |V_k|\, B_{ik}^{ii}\, \frac{\Delta V_k}{V_k} \quad (36)$$

Then, omit from B, those network elements that affect MVAR flows and the angle shifting effects of phase shifters. Divide Equation (35) and (36) by $|Vi|$, assume $V_k$= 1.0*pu* and also neglecting series resistance in calculating the elements in *B.*

$$\Delta P_i = B\, \Delta\delta \quad (37)$$

$$\frac{\Delta\, Q_i}{|V_i|} = B_{ii}\, \Delta V = V \quad (38)$$

$$\Delta P_1 = P_{G1} - P_{L1} - P_{T1} \quad (39)$$

$$\Delta Q_1 = Q_{G1} - Q_{L1} - Q_{T1} \quad (40)$$

$$P_{Ti} = \sum_{j=1}^{n} \left( V_1\, V_j\, Y_{1j}\, \cos\left(\delta_i - \delta_j - v_{ij}\right) \right) \quad (41)$$

$$Q_{Ti} = \sum_{j=1}^{n} \left( V_1\, V_j\, Y_{ij}\, \sin\left(\delta_i - \delta_j - v_{ij}\right) \right) \quad (42)$$

For the H submatrix

$$H_{ij\ (i\neq j)} = \frac{\partial \Delta P_1}{\partial \delta_j} = V_i y_{ij}\, \sin\left(\delta_1 - \delta_j - v_{ij}\right) \quad (43)$$

$$H_{ij} = \frac{\partial \Delta P_1}{\partial \delta_j} = \sum_{j=1, J\neq 1}^{n} V_i y_{1J} V_J\, \sin\left(\delta_1 - \delta_3 - v_{ij}\right) \quad (44)$$

For the N submatrix:

$$N_{ij\ (i\neq j)} = -V_J\, \frac{\partial \Delta P_1}{\partial \delta_j} = V_i y_{ij} V_J \cos\left(\delta_1 - \delta_j - v_{ij}\right) \quad (45)$$

$$N_{ij} = -V_1\, \frac{\partial \Delta P_1}{\partial V_j} = \sum_{j=1}^{n} V_1 y_{ij} V_J\, \cos\left(\delta_1 - \delta_j - v_{ij}\right) + V_1 y_{ij} V_J\, \cos\left(\delta_1 - \delta_j - v_{ij}\right) \quad (46)$$

For the J submatrix:

$$J_{ij\ (i\neq j)} = -\frac{\partial \Delta Q_1}{\partial \delta_j} = V_i y_{ij} V_J \cos\left(\delta_1 - \delta_j - v_{ij}\right) \quad (47)$$

$$J_{ij} = -V_1\, \frac{\partial \Delta Q_1}{\partial V_j} = \sum_{j=1}^{n} V_1 y_{ij} V_J\, \cos\left(\delta_1 - \delta_j - v_{ij}\right) + V_1 y_{ij} V_J\, \cos\left(\delta_1 - \delta_j - v_{ij}\right) \quad (48)$$

For the L submatrix:

$$L_{ij\ (i\neq j)} = -\frac{\partial \Delta Q_i}{\partial \delta_j} = V_i y_{ij} V_J \cos\left(\delta_1 - \delta_j - v_{ij}\right) \quad (49)$$

$$J_{ij} = -V_1\, \frac{\partial \Delta Q_i}{\partial V_j} = \sum_{j=1}^{n} V_1 y_{ij} V_J\, \cos\left(\delta_1 - \delta_j - v_{ij}\right) + V_1 y_{ij} V_J\, \cos\left(\delta_1 - \delta_j - v_{ij}\right) \quad (50)$$

Where

$\boldsymbol{Y_{Bus}}$ = Admittance matrix; $\boldsymbol{Z_{Bus}}$ = Impedence matrix; $\boldsymbol{R_o}$ = Per-Kilometre Active Resistance; $\boldsymbol{\mathcal{L}}$ = design resistivity of conductor (in *Q, m*); ***A*** = cross-sectional area of conductor (in $m^2$); $\boldsymbol{x_o}$ = Per-Kilometre Inductive Reactance; $\boldsymbol{b_o}$ = Per-Kilometre Capacitive Susceptance; ***r*** = conductor radius in meter (m); $\boldsymbol{D_{GMD}}$ = geometric mean distance between phase conductors; ***D*** = spacing between the conductors; $\boldsymbol{P_D}$ = Active Power on feeder; ***CLD*** = Complex load demand; ***pf*** = Power factor; ***TC*** = Transformer Capacity; $\boldsymbol{L^T}$ = Percentage Loading on transformer; $\boldsymbol{V_D}$ = voltage drop; $\boldsymbol{I^F}$ = Average Current on Feeder; ***Z*** = Impedance of feeder; ***K*** = transformation ratio; $\boldsymbol{V_1}$ & $\boldsymbol{V_2}$ = primary voltage and secondary voltage; $\boldsymbol{N_1}$ & $\boldsymbol{N_2}$ = number of turns on primary and secondary side of transformer; $\boldsymbol{T_c}$ = compensation capacitor/capacitor bank size in Kvar; ***P*** = real power; ***Ui*** = lagging reactive Power; ***Ti*** = apparent power at a lagging power factor; $\boldsymbol{N_{bus}}$ = Number of bus candidates; $\boldsymbol{x_i}$ = 0/1, 0 means no capacitor installed at bus *i;* $\boldsymbol{C_{0i}}$ = Installation cost; $\boldsymbol{C_{1i}}$ = Per Kvar cost of capacitor banks; $\boldsymbol{S_i}$ = Complex power injected into an *i-th* bus of a power system; $\boldsymbol{S_i^*}$ = Conjugate complex power; $\boldsymbol{V_i}$ = voltage at the *i-th* bus with respect to ground; $\boldsymbol{I_i}$ = source current injected into the bus; $\boldsymbol{P_i}$ = Real power; $\boldsymbol{Q_i}$ = Reactive power; $\boldsymbol{\Delta P}$ = changes in real Power; $\boldsymbol{\Delta Q}$ = changes in reactive power; $\boldsymbol{\Delta V}$ = changes in voltage magnitude; $\Delta\delta$ = changes in phase angle of voltage; $\boldsymbol{B_{ik}}$ and $\boldsymbol{B_{ik}}$ = elements of $-B_{jk}$ matrix; $\boldsymbol{C_{2i}}$ = Operating cost of per bank yearly; $\boldsymbol{C_E}$ = Cost of each KWh loss, in \$/kWh; $\boldsymbol{B_i}$ = Number of capacitor banks; ***M*** = Planning period (years); $\boldsymbol{M_1}$ =Time duration, in hours, of load level; $\boldsymbol{P_L^1}$ = Total system loss at load level; $\boldsymbol{V_{Stab}}$ = Voltage instability; $\boldsymbol{P_L}$ = power transfer over a lossless line/ power transferred per phase; ***X*** = transfer reactance per phase; $\boldsymbol{\delta}$ = phase angle between ***Es*** and *Vr*; ***Es*** = sending end voltage; ***Vr*** = receiving end voltage; $\emptyset$ = the rotor angle displacement of the machine, which defines angular instability

## 4 RESULTS AND DISCUSSIONS

The results of the voltage stability studies of the PHED in Ikwerre Road, Diobu, Port Harcourt are presented in the section. ETAP software was used for the simulation and analysis of the supply network to the study area. Table 3 shows The outcome of increasing the DG size on voltages of different load points. Table 4 demonstrates the effect of increasing the size of the DG unit on power flow. Table 5 demonstrates the effect of increasing the size of the DG unit on power flow. Table 6 demonstrates the effect of increasing the size of the DG unit on power flow. Table 7 shows increasing DG to maximum load capacity. Table 8 shows the losses on the power system components. Figure 6 shows The outcome of increasing the DG size on voltages of different load points due to the fast voltage stability index rate. Figure 7 shows The outcome of increasing the DG size on voltages of different load points due to line stability index rate. Figure 8 shows The outcome of increasing the DG size on voltages of different load points due to line stability factor. Figure 9 shows the compensated power supply system to Ikwerre Road, Diobu, Port Harcourt.

From Table 3, the effect of an increasing size of DG on voltages of each bus indicates that the voltage stability of each bus is more enhanced. The penetration of voltage stability indices values with different DG sizes established that the line, which starts from bus 30 to bus 33 is the weakest. So, the DG unit is installed at bus 33. The DG size is varied from 0 to 50% from load to display the effect of the DG size on Voltage Stability Indices. The values of voltage stability indices at each line are nearer to zero when installing the DG unit in bus 33. So, voltage stability is enhanced at each bus.

From Table 4, it is observed that real & reactive power generated by PHCN is reduced due to installing the DG unit at bus 33. Furthermore, power losses get reduced obviously. But when DG size reaches a certain size power losses are increased. From the result analysis, optimum DG size is needed to limit the best DG size to get the best minimization power losses. From Table 5, real & reactive power generated by PHCN is reduced due to install the DG unit at bus 11. Furthermore, power losses get reduced obviously. But when DG size reaches a certain size power loss is increased. From the result analysis, optimum DG size is needed to limit the best DG size to get the best minimization power losses. From Table 6, real power generated by PHCN was reduced due to install the DG unit at bus 30. While there is an increase in the reactive power generated by PHCN and the total load due to improving the voltage of each bus. Furthermore, power losses get reduced but when reach certain DG size active and reactive power losses increased. Figure 4 demonstrates the effect of an increasing size of DG on active and reactive power losses and Figure 5 shows the effect of the increasing size of the DG unit on the P-V curve of each bus.

Table 7 demonstrates the effect of increasing the size of the DG unit on the maximum value of the loading parameter of the power system. The maximum value of the loading parameter of the power system increased when increasing the size of DG. Maximum load ability changes from 3.1217 to 4.0125 when the DG generates 60% from the load. Maximum load ability is developed by 0.8908. This change shows that Maximum load ability enhanced due to install DG.

Due to the voltage instability existing, the power supply network was compensated with the integration of 0.02MVAR capacity of a capacitor bank (power electronics controller) to improve the power quality (see Figure 9). A significant voltage drop was noticed at each bus in the network, a lower than the declared statutory IEEE regulation, before compensation and after compensation with 0.02MVAR reactive power. This improved the network in terms of quality and reliability. Also, the capacity of 0.02 MVAR compensation capacitor to the 11KV distribution networks, buses strongly improved the system stability, losses and also reduced the system performance to barest and acceptable operating conditions (see Figure 6 – 8).

**Table 3: Outcome of Voltage at each bus due to the increasing size of the DG**

| Voltage Bus | Without DG | DG 10 % of load | DG 20 % of load | DG 30 % of load | DG 40 % of load | DG 50 % of load | DG 60 % of load |
|---|---|---|---|---|---|---|---|
| Voltage at Bus 1 | 1 | 1 | 1 | 1 | 1 | 1 | 1 |
| Voltage at Bus 2 | 0.997032 | 0.997357 | 0.997669 | 0.997969 | 0.998259 | 0.99854 | 0.998807 |
| Voltage at Bus 3 | 0.982938 | 0.98500 | 0.986979 | 0.988884 | 0.990724 | 0.992504 | 0.994200 |
| Voltage at Bus 4 | 0.975457 | 0.978801 | 0.982011 | 0.985102 | 0.988087 | 0.990975 | 0.993726 |
| Voltage at Bus 5 | 0.968063 | 0.972738 | 0.977229 | 0.981553 | 0.985728 | 0.989769 | 0.993617 |
| Voltage at Bus 6 | 0.949662 | 0.957688 | 0.965392 | 0.97281 | 0.979971 | 0.986898 | 0.993502 |
| Voltage at Bus 7 | 0.946174 | 0.954233 | 0.961967 | 0.969412 | 0.976599 | 0.983551 | 0.990178 |
| Voltage at Bus 8 | 0.941331 | 0.949432 | 0.957206 | 0.96469 | 0.971912 | 0.978982 | 0.985559 |
| Voltage at Bus 9 | 0.935063 | 0.94322 | 0.951047 | 0.95858 | 0.96585 | 0.972883 | 0.979584 |
| Voltage at Bus 10 | 0.929415 | 0.937623 | 0.945498 | 0.953076 | 0.960389 | 0.967462 | 0.974202 |
| Voltage at Bus 11 | 0.928544 | 0.93676 | 0.944642 | 0.952227 | 0.959547 | 0.966626 | 0.973372 |
| Voltage at Bus 12 | 0.927045 | 0.935274 | 0.943169 | 0.950766 | 0.958097 | 0.965187 | 0.971943 |
| Voltage at Bus 13 | 0.920933 | 0.929217 | 0.937163 | 0.94481 | 0.952187 | 0.959322 | 0.966121 |
| Voltage at Bus 14 | 0.918667 | 0.926971 | 0.934937 | 0.942602 | 0.949996 | 0.957147 | 0.963967 |
| Voltage at Bus 15 | 0.917255 | 0.925572 | 0.933558 | 0.941226 | 0.948631 | 0.955793 | 0.962615 |
| Voltage at Bus 16 | 0.915887 | 0.924217 | 0.932206 | 0.939893 | 0.947309 | 0.954481 | 0.961313 |
| Voltage at Bus 17 | 0.913864 | 0.922208 | 0.930215 | 0.937918 | 0.94535 | 0.952536 | 0.959382 |
| Voltage at Bus 18 | 0.913253 | 0.921607 | 0.929619 | 0.937327 | 0.944763 | 0.951954 | 0.958804 |
| Voltage at Bus 19 | 0.996503 | 0.996829 | 0.997141 | 0.997441 | 0.997732 | 0.998012 | 0.998285 |

| | | | | | | | |
|---|---|---|---|---|---|---|---|
| Voltage at Bus 20 | 0.992926 | 0.993252 | 0.993565 | 0.993867 | 0.994158 | 0.994443 | 0.994709 |
| Voltage at Bus 21 | 0.992221 | 0.992548 | 0.992861 | 0.993163 | 0.993455 | 0.993737 | 0.994005 |
| Voltage at Bus 22 | 0.991584 | 0.991911 | 0.992224 | 0.992526 | 0.992818 | 0.993145 | 0.993369 |
| Voltage at Bus 23 | 0.979352 | 0.981421 | 0.983408 | 0.98532 | 0.987167 | 0.988954 | 0.990656 |
| Voltage at Bus 24 | 0.972681 | 0.974765 | 0.976765 | 0.97869 | 0.98055 | 0.982349 | 0.984062 |
| Voltage at Bus 25 | 0.969356 | 0.971447 | 0.973454 | 0.975386 | 0.977252 | 0.979057 | 0.980776 |
| Voltage at Bus 26 | 0.94773 | 0.956452 | 0.964823 | 0.972882 | 0.980662 | 0.98819 | 0.995365 |
| Voltage at Bus 27 | 0.945167 | 0.954858 | 0.96416 | 0.973116 | 0.981763 | 0.99013 | 0.998103 |
| Voltage at Bus 28 | 0.933727 | 0.947672 | 0.961059 | 0.973948 | 0.986391 | 0.998433 | 1.009915 |
| Voltage at Bus 29 | 0.925509 | 0.942667 | 0.959137 | 0.974998 | 0.99031 | 1.005128 | 1.019262 |
| Voltage at Bus 30 | 0.921952 | 0.940826 | 0.958946 | 0.976394 | 0.993241 | 1.009545 | 1.025094 |
| Voltage at Bus 31 | 0.917791 | 0.936749 | 0.954947 | 0.972468 | 0.989382 | 1.005749 | 1.021356 |
| Voltage at Bus 32 | 0.916875 | 0.935852 | 0.954067 | 0.971604 | 0.988533 | 1.004913 | 1.020533 |
| Voltage at Bus 33 | 0.916591 | 0.935574 | 0.953794 | 0.971336 | 0.98827 | 1.004655 | 1.020279 |

**Table 4: The outcome of increasing the DG size on power flow**

| DG% | P intake MWatt | Qintake MVAR | MWatt | MVAR | Pl MWatt | Ql MVAR | Plosses KWatt |
|---|---|---|---|---|---|---|---|
| 0% | 3.91753 | 2.4351 | 1 | 1 | 3.715 | 2.3 | 202.5 |
| 10% | 3.4891 | 2.1673 | 0.3715 | 0.23 | 3.715 | 2.3 | 145.6 |
| 20% | 3.07737 | 1.9112 | 0.746 | 0.46 | 3.715 | 2.3 | 105.4 |
| 30% | 2.680467 | 1.6653 | 1.1145 | 0.69 | 3.715 | 2.3 | 80 |
| 40% | 2.29687 | 1.4288 | 1.486 | 0.92 | 3.715 | 2.3 | 67.9 |
| 50% | 1.92529 | 1.2 | 1.8575 | 1.15 | 3.715 | 2.3 | 67.8 |
| 60% | 1.5733 | 0.9798 | 2.22 | 0..4 | 3.715 | 2.3 | 78.3 |



**Table 5: The outcome of increasing the DG size to the maximum load ability**

| Rating of installed DG | Max. Load Ability | Active Power (MWatt) | Reactive Power (MVAR) |
|---|---|---|---|
| 0% from the load | 3.1217 | | |
| 10% from the load | 3.2365 | 0.064328 | 0.026238 |
| 20% from the load | 3.4785 | 0.126472 | 0.052477 |
| 30% from the load | 3.6754 | 0.189708 | 0.078715 |
| 40% from the load | 3.7984 | 0.252944 | 0.104953 |
| 50% from the load | 3.8659 | 0.31618 | 0.131191 |
| 60% from the load | 4.0125 | 0.379416 | 0.157429 |

**Table 6: The outcome power flow as a result of increasing different DG size**

| DG% | P intake MWatt | Q intake MVAR | Pdg MWatt | Qdg MVAR | Pl MWatt | Ql MVAR | Plosses KWatt |
|---|---|---|---|---|---|---|---|
| 0% | 6.3236 | 2.6238 | 0 | 0 | 6.22 | 2.6 | 94 |
| 10% | 5.6629 | 2.1604 | 0.6323 | 0.2623 | 6.22 | 2.6 | 66 |
| 20% | 5.0087 | 1.7364 | 1.2647 | 0.5247 | 6.22 | 2.6 | 44 |
| 30% | 4.3604 | 1.3483 | 1.8970 | 0.7871 | 6.22 | 2.6 | 28 |
| 40% | 3.7174 | 0.9930 | 2.5294 | 1.0495 | 6.22 | 2.6 | 17 |
| 50% | 3.0794 | 0.6683 | 3.1618 | 1.3119 | 6.22 | 2.6 | 12 |
| 60% | 0.244611 | 0.03718 | 0.37941 | 0.157429 | 6.22 | 2.6 | 11.27 |
| 70% | 0.181711 | 0.01020 | 0.44265 | 0.183667 | 6.22 | 2.6 | 14.6 |

**Table 7: The outcome of the power flow of increasing different DG size on load point**

| Rating | P intake (MWatt) | Q intake (MVAR) | $P_{DG}$ (MWatt) | $Q_{DG}$ | $P_l$ (MWatt) | $Q_l$ (MVAR) | Plosses (KWatt) | Qlosses (MVAR) |
|---|---|---|---|---|---|---|---|---|
| Without DG | 3.765 | 1.785 | 0 | 0 | 3.684 | 1.718 | 161 | 107 |
| 10% | 3.432 | 1.867 | 0.371 | 0 | 3.688 | 1.781 | 129 | 86 |
| 20% | 3.047 | 1.918 | 0.743 | 0 | 3.691 | 1.844 | 109 | 73 |
| 30% | 2.598 | 1.977 | 1.114 | 0 | 3.694 | 1.909 | 98 | 67 |
| 40% | 2.295 | 2.042 | 1.486 | 0 | 3.697 | 1.974 | 97 | 68 |
| 50% | 1.893 | 2.115 | 1.857 | 0 | 3.699 | 2.040 | 105 | 75 |

**Table 8: Power systems component and losses**

| Components | losses, MW (without) | losses, MW(with) | losses, Mvar (without) | losses, Mvar (without) 2 |
|---|---|---|---|---|
| transformer,T1 | 0.07 | 0.072 | 0.045 | 0.035 |
| transformer,T2 | 0.07 | 0.072 | 0.045 | 0.035 |
| cable1 | -0.143 | -0.144 | -0.089 | -0.07 |
| cablee2 | 0.107 | 0.109 | 0.067 | 0.048 |
| transformer,T4 | 0.036 | 0.036 | 0.022 | 0.022 |
| cable3 | 0.0107 | 0.109 | 0.067 | 0.048 |
| cable4 | 0.071 | 0.072 | 0.022 | 0.024 |
| transformer,T5 | 0.037 | 0.037 | 0.067 | 0.023 |
| cable5 | 0.071 | 0.072 | 0.044 | 0.024 |
| cable6 | 0.033 | 0.034 | 0.023 | 0.001 |
| transformer, 7 | 0.037 | 0.037 | 0.044 | 0.023 |
| cable8 | 0.033 | 0.034 | 0.023 | 0.001 |
| tranformer,T9 | 0.003 | 0.004 | 0.044 | -0.017 |
| cable9 | 0.003 | 0.03 | 0.023 | 0.018 |
| cable10 | 0.003 | 0.003 | 0.044 | -0.017 |



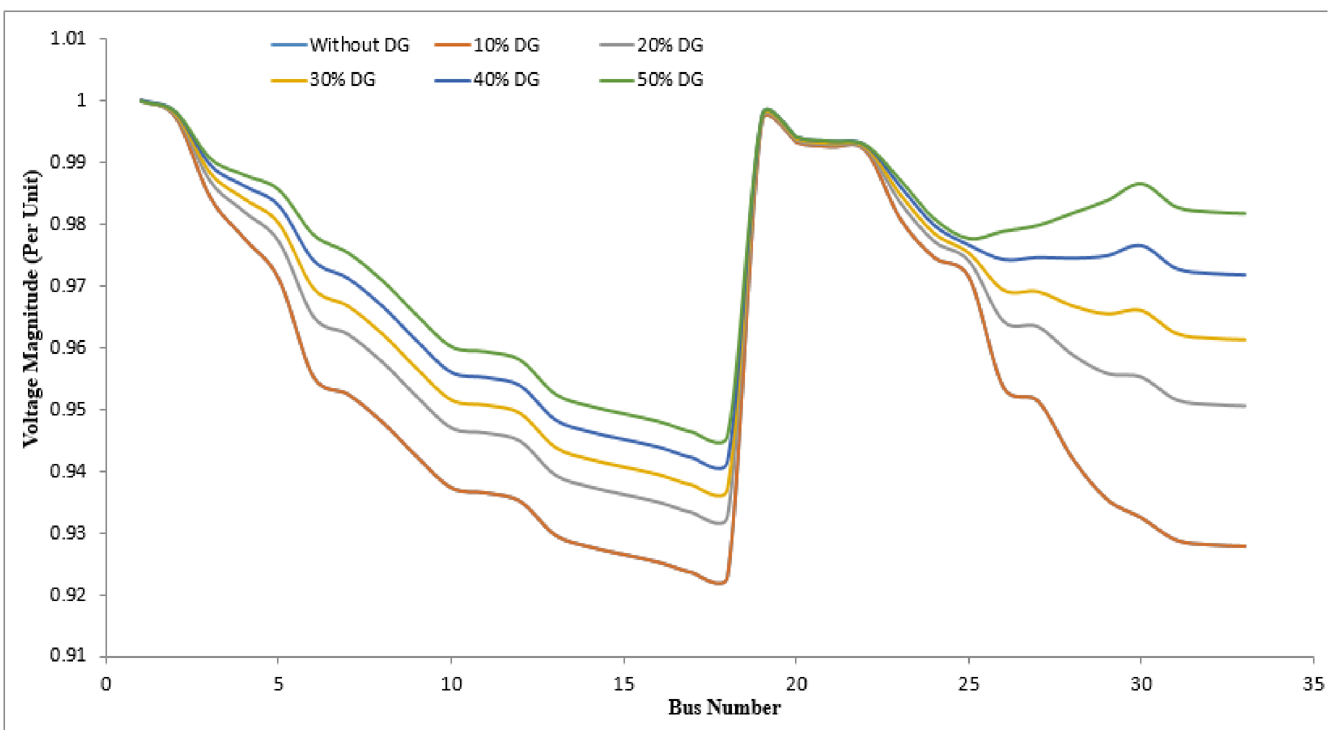


**Figure 4: The outcome of increasing the DG size on the voltage of each load point**

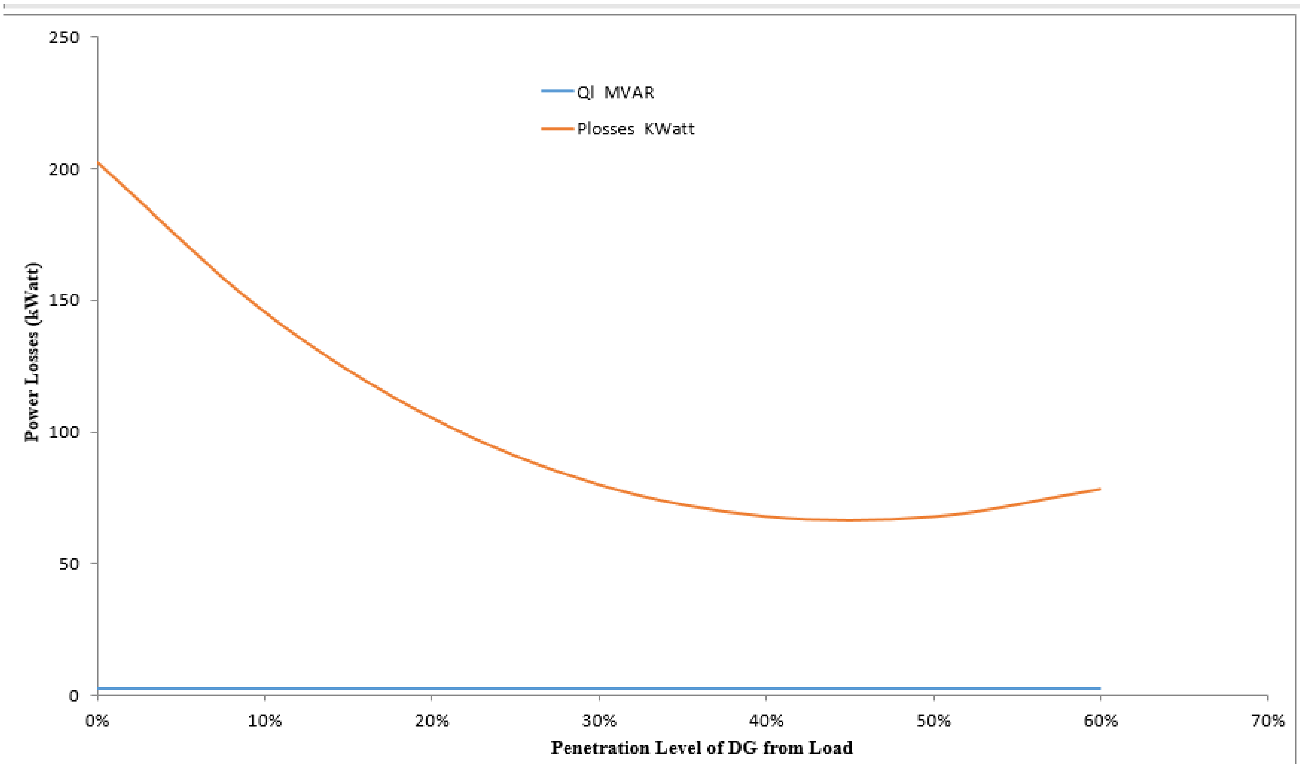


**Figure 5: P-V curve showing the outcome of increasing the DG size due to power losses**

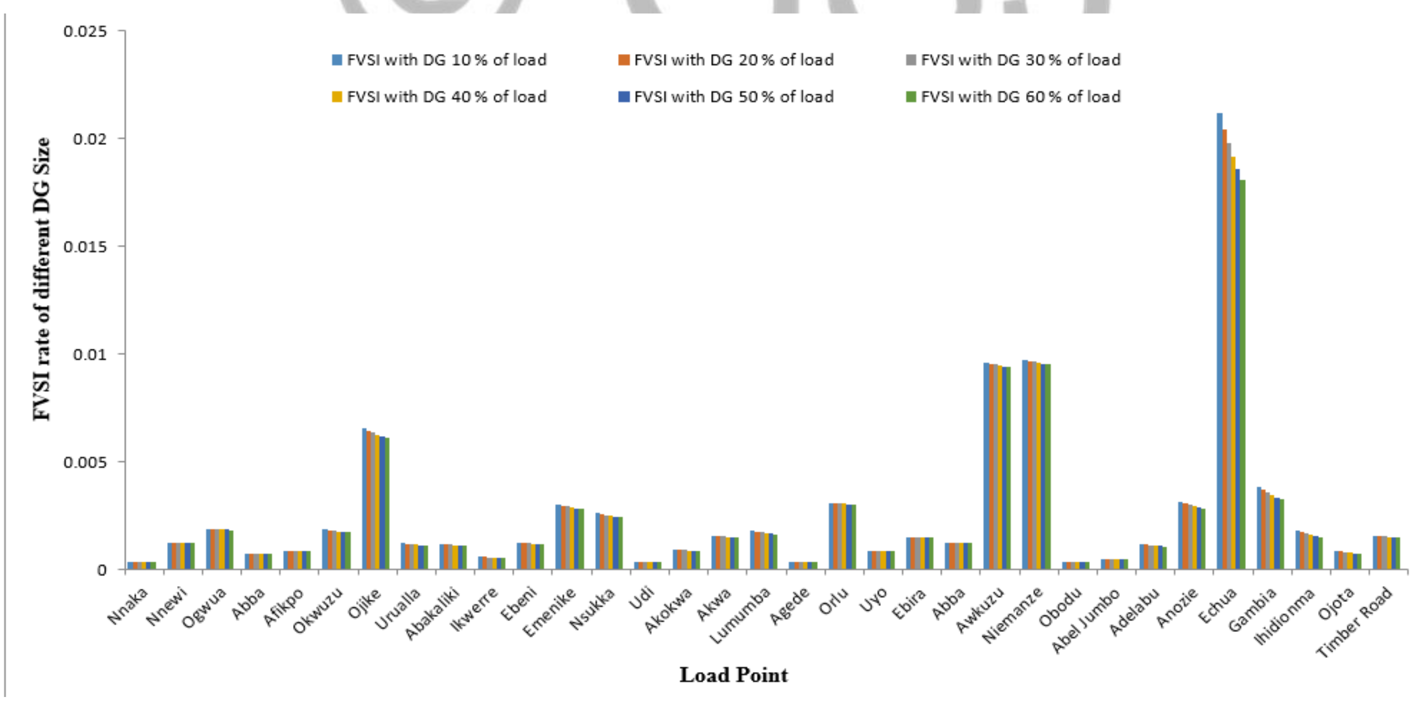


**Figure 6: Values of different DG size due to the fast voltage stability index (FVSI)**

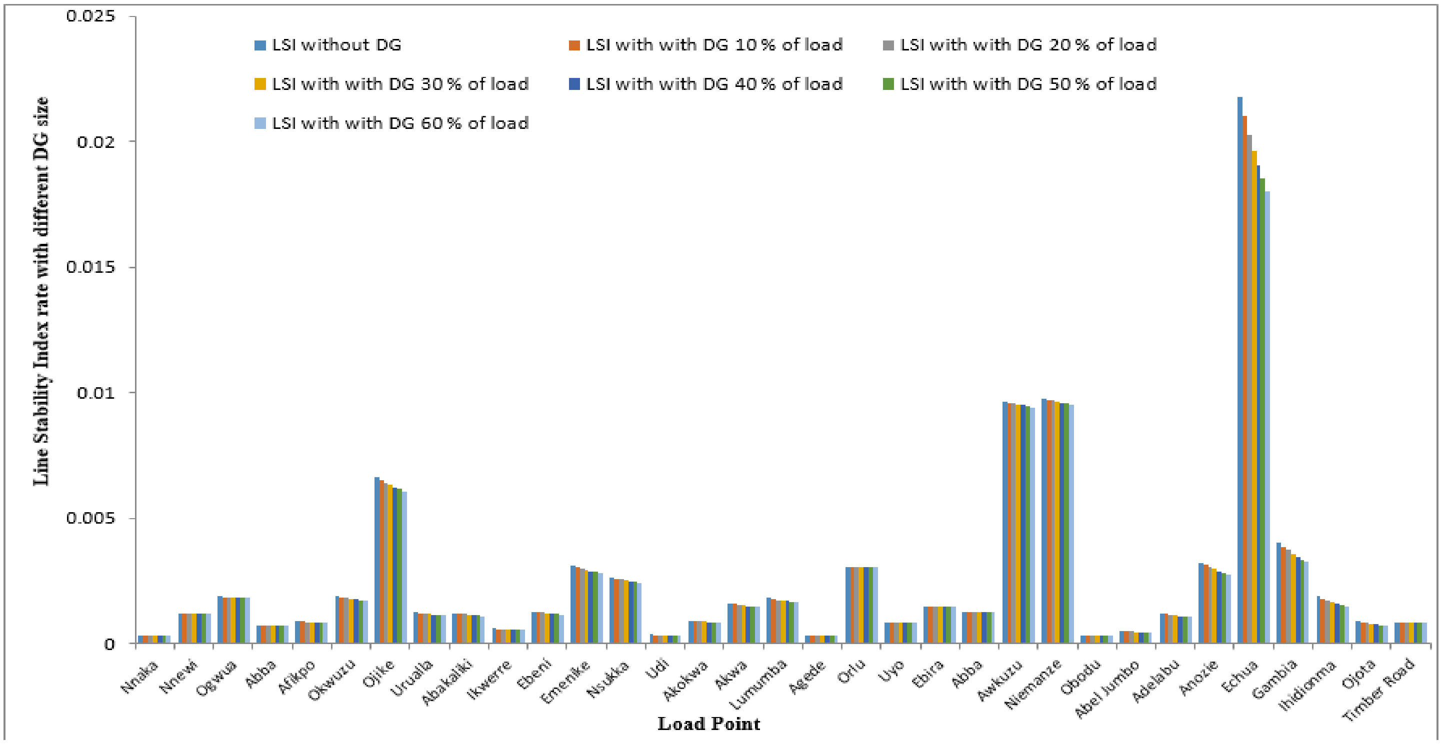


**Figure 7: Values of different DG size due to Line Stability Index (LSI)**

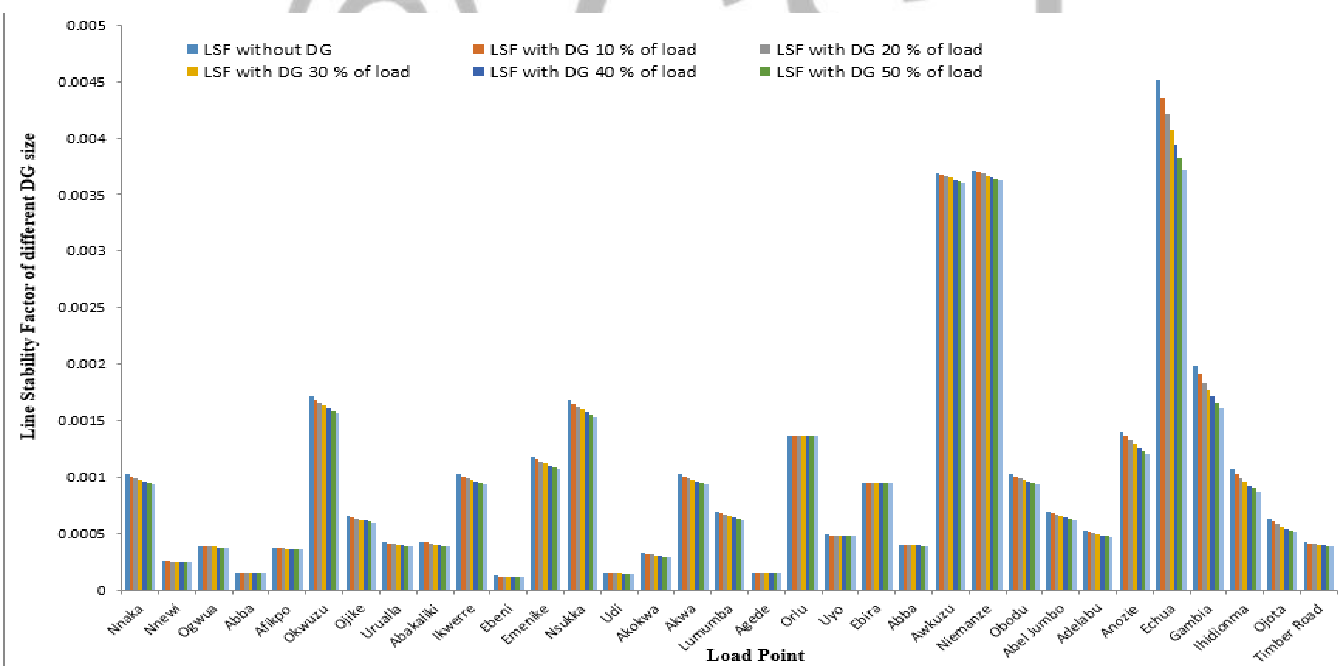


**Figure 8: Values of different DG size due to Line Stability Factor (LSF)**

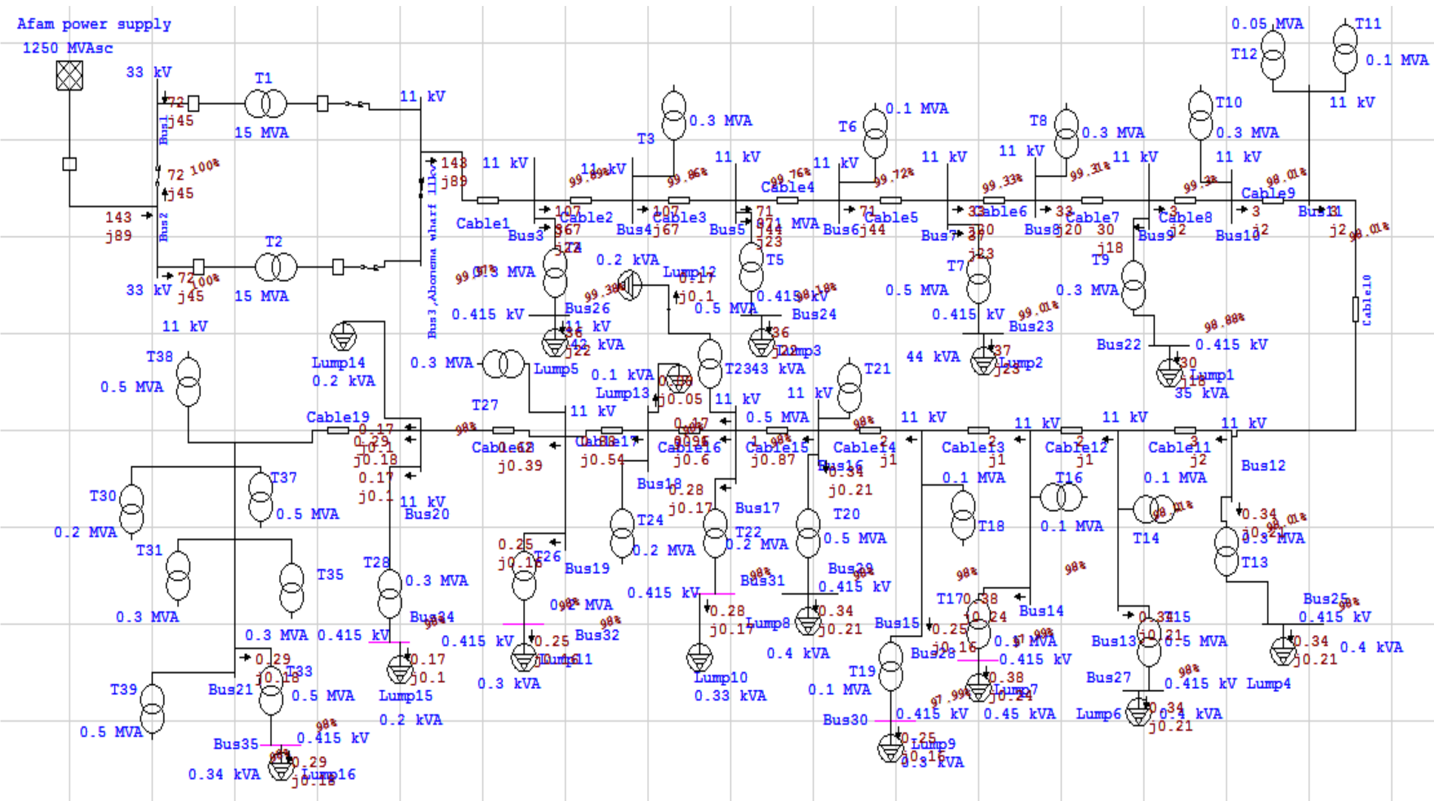


Figure 9 the power supply system to Ikwerre Road, Diobu (Compensated)

## 5 CONCLUSION

This research conducted voltage stability studies of the PHED to Ikwerre Road, Diobu, Port Harcourt. From the power flow analysis on the Ikwerre Road 11KV distribution network, it was observed that the network is highly overloaded and not frequently maintained, which resulted in a drastic drop in voltage profile and excessive power loss. A solution to the high rate of voltage instability on a regular pattern is necessary to alleviate and avoid excessive loading on the distribution network and also consider and determine the capacity of the transformer, cables, and other components, otherwise, there may be system breakdown. In this research, the total power loss in the 11KV distribution network in the Ikwerre Road is compensated to reduce the voltage drop in the feed and buses. The introduction of values of the fast voltage stability index (FVSI), line stability index (LSI), line stability factor (LSF) at the diverse DG and the effect of the increasing size of DG on power flow at residential load gave rise to improvements in both the voltage profile of the network and reduction in losses. The maximum value of the loading parameter of the power system increased when increasing the size of DG. The demonstration of increasing the size of the DG unit on power flow was observed that there is a reduction in real power generated PHCN due to install the DG unit at Gambia street. Results showed that the losses were reduced significantly and the average voltage drop reduces to acceptable operating conditions. This means that for the same power injected into the network more real power load can be accommodated to support injection substation capacity and performance. It is observed that the capacitors operating cost during the planning period increases with time but cannot be compared to the increase in profit and cost-saving as a result of loss reduction over the same period. The research shows significantly improve power quality, power factor, and system voltage stability in the study area. Power system planners and operators can consider the result of this research to safeguard and ensure efficient power delivery from regular outages in the network. The solution to loss minimization and optimum generation cost on the power grid is beneficial to the economic activities of the Ikwerre Road, Diobu axis of Port Harcourt

## REFERENCES

[1] O. Athe, D. C. Idoniboyeobu, and S. L. Braide, "Optimization of generation cost for economic operation of Sapele thermal power plant using particle swarm optimization (PSO) method," *American Journal of Engineering Research (AJER),* Vol. 9, no. 12, pp. 167-179, 2020. Available at https://www.academia.edu/45035202/Optimization_of_Generation_Cost_for_Economic_Operation_of_Sapele_Thermal_Power_Plant_using_Particle_Swarm_Optimization_PSO_Method

[2] E.C. Obuah and T.O.J. Alalibo, "Techno-Economic Analysis of hybrid photovoltaic/diesel energy system for oil and gas industries in Nigeria," *International Journal of Science and Research (IJSR)*, vol. 6, no. 7, pp. 346 – 351, 2017.

[3] T. Archana, "*What is voltage stability in power system? definition, types & calculation of voltage stability limit*," Circuit Globe, 2016, July 19 [Online] Available at https://circuitglobe.com/voltage-stability-in-power-system.html [Accessed: 06- Feb- 2021]

[4] A. N. Ezeala, D. C. Idoniboyeobu, and S. L. Braide, "Analysis of 11kV, Obi-Wali, Rumuigbo Distribution Network for improved performance using predictive reliability assessment method," *American Journal of Engineering Research (AJER),* Vol. 9, no. 12, pp. 132-145, 2020. Available at https://www.academia.edu/45034877/Analysis_of_11kV_Obi_Wali_Rumuigbo_Distribution_Network_for_Improved_Performance_using_Predictive_Reliability_Assessment_Method

[5] UK Essays, "*Major causes of voltage instability*," UKEssays.Com. November 2018 [Online]. Available at https://www.ukessays.com/essays/engineering/major-causes-of-voltage-instability-engineering-essay.php?vref=1 [Accessed: February 2, 2021]

[6] N. Palukuru, S. H. nee Dey, T. Datta, and S. Paul, "Voltage stability assessment of a power system incorporating FACTS controllers using unique network equivalent," *Ain Shams Engineering Journal*, vol. 5, no. 1, pp. 103-111, 2014

[7] I. K. Okakwu, E. A. Ogujor and P. A. Oriaifo, "Load flow assessment of the Nigerian 330kV power system," *American Journal of Electrical Engineering*, vol. 5, no. 4, pp. 1-6, 2017

[8] O. S. Onohaebi and Y. O. Lawal, "Poor maintenance culture; the bane to electric power generation in Nigeria," *Journal of Economics and Engineering*, vol. 1, no. 20, pp. 28-46, 2010.

[9] S. R. Islam, D. Sutanto and K. M. Muttaqi, "Coordinated decentralized emergency voltage and reactive power control to prevent long-term voltage instability in power system," *In IEEE transactions on power systems*, vol. 30, No. 5, pp. 2591-2603, sept 2015

[10] M. Amroune, T. Bouktir and I. Musirin, "Power system voltage instability risk mitigation via emergency demand response-based whale optimization algorithm," *Protection and control of modern power systems*, vol. 4, no. 25, 2019. https://doi.org/10.1186/s41601-019-0142-4

[11] T. O. J. Alalibo, S. Orike, and P. Elechi, "Efficient bandwidth allocation in wireless network using whale optimization algorithm," *Journal of Newviews in Engineering and Technology (JNET)*, vol. 2, no. 1, pp. 97 – 101, 2020

[12] K. L. Prasanna, A. Jain and R. J. Kumar, "Optimal distributed generation placement using a hybrid technique," *IEEE PES Asia-Pacific Power and Energy Engineering Conference (APPEEC), Bangalore*, vol. 13, no. 23, pp. 1-6, 2017

[13] D. Zimmerman, and H. Chiang, "Fast decoupled power flow for unbalanced radial distribution systems" *IEEE Transactions on Power Systems*, vol. 10, no. 4, pp. 2045-2052, 1995

[14] O. Afolabi, W. Ali, P. Cofie, J. Fuller, P. Obiomon and E. Kolawole, "Analysis of the load flow problem in power system planning studies," *Energy and Power Engineering,* vol. 7, no. 10, pp. 509-523, 2015.

[15] I. J. Kothari and D. P. Nagrath, *Modern power system analysis*, 3rd Ed. New York, 2007.

[16] S. Kriti, "Comparison between load flow analysis methods in power system using MATLAB," *International Journal of Scientific & Engineering Research*, vol. 5, no. 5, pp.1-8, 2014

[17] S. Ghosh and D. Das, "Method for load-flow solution of radial distribution networks," IEE Proceedings-Generation, Transmission and Distribution, vol. 146, no. 6, pp. 643-648, 1999

[18] W. F. Tinney and C. E. Hart, "Power flow solution by Newton's method," *IEEE Transactions on Power. Apparatus and Systems*, vol. 86, no. 196, pp. 1449-1460, 2016

[19] J. Jayaprakash, P. M. Angelin, R. Jothilakshmi and P. J. Juanola, "Planning and coordination of relay in distribution system using ETAP," *Pakistan Journal of Biotechnology*, vol. 13, no. 5, pp. 252-256, 2016.